An FDD/FD Capable, Single Antenna RF Front End from 800MHz to 1.2GHz w/ Baseband Harmonic Predistortion

Hazal Yüksel, Thomas Tapen, Zachariah Boynton, Emory Enroth, Alyssa Apsel, Alyosha C. Molnar
Department of Electrical and Computer Engineering, Cornell University, 14853, Ithaca, NY, USA

***Abstract* — A highly-integrated dual technology (28nm and 130nm SOI) widely tunable software-defined RF duplexing front-end for FDD, FD, and TDD applications is presented. Predistortion and harmonic upconversion are used to cancel second and third harmonics generated by PA nonlinearity by up to 30 dB. A novel form of non-reciprocal, distributed degeneration is used to suppress TX noise that desensitizes the RX for full duplex operation. The distributed degeneration network improves RX noise figure by 7dB over baseline TX operation for same channel TX-RX. The transceiver achieves a 23dBm output power while maintaining more than 30dB of TX-RX isolation over the 0.8-1.2GHz band.**

***Index Terms* — full-duplex, transceiver, distributed, TX-RX isolation, non-reciprocity, software defined radio, degeneration**

I. Introduction

Truly flexible, integrated RF front ends will need to support a variety of duplex scenarios including TDD, FDD, and likely single channel full duplex (FD). The front end must function over a range of RX/TX frequencies and spacings, while meeting spectral mask requirements and suppressing TX signals, distortion, harmonics, and noise at the RX port. Same channel FD is particularly challenging due to self-interference (SI), requiring SI cancellation across the RF, analog and digital domains [1]. Ideally, this is accomplished without costly off-chip filters, diplexers or circulators, and also using a single antenna interface such as in [2] or [3]. In this paper we present a dual technology duplexing front-end, similar to [4], that supports TDD, FDD, and FD while implementing predistortion to suppress spurious TX emissions, and spurious emissions at harmonics of the TX frequency. Our design combines a programmable complex-weighted distributed transmitter whose subtransmitters tap into an LC based transmission line. A non-reciprocal distributed PA degeneration network suppresses signal and noise of individual transmitters at the receiver, including when RX and TX are closely spaced or identical.

II. System Discussion

Fig. 1 shows the block diagram of our distributed duplexer. As in [4], complex weighting of baseband TX signals before upconversion provides suppression at the RX while maximizing signal at the antenna port. In FDD mode transmitter noise is suppressed at the receiver frequency with frequency-selective degeneration. Compared to [4], this system offers a number of improvements. First, we take advantage of the speed and compactness of 28nm CMOS for LO and mixer circuits while implementing the high output voltage PAs and high-Q passives of the transmission line in an SOI process, splitting the design between two chips. The SOI process offers low substrate loss, therefore reducing the loss of the transmission line inductors. A new mode of operation, FD mode, is enabled by the distributed degeneration network. Low distortion transmission is enabled by the addition of harmonic suppression both for spectral mask compliance and to avoid saturating the RX. The architecture employs 15 8-phase passive mixers with associated circuitry, driven by two LO chains (RX and TX) to implement the following capabilities:

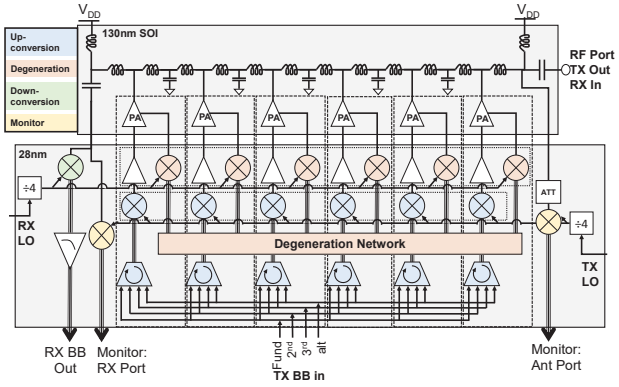

Fig. 1. System block diagram.

A. Mixer Dynamic Range Improvements

Proper operation of frequency-selective degeneration requires that degeneration mixers support the large RF signal swings that may be present due to the TX signal. As swing on the RF port becomes large, it may drive the source terminals to low enough voltage to turn mixer transistors on even when their gates are "off", degrading performance. To mitigate this effect, the LO pulse generators driving mixer gates were designed to drive

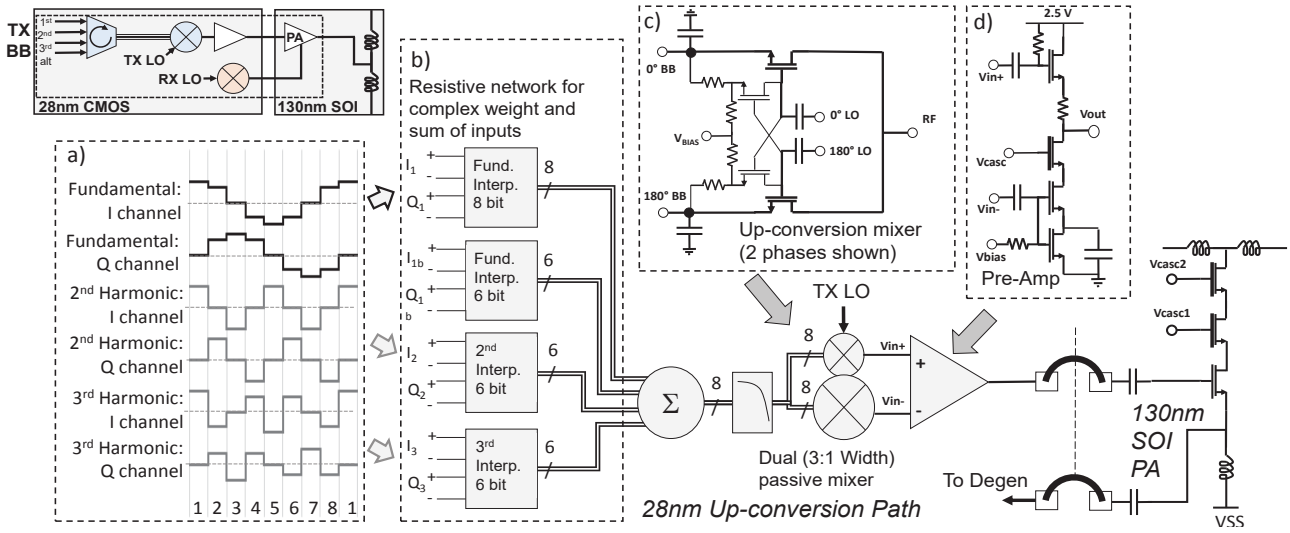

Fig. 2. The upconversion chain.

the gates below the DC voltages of the RF and baseband ports while still driving the mixers' gates to their maximum allowable voltage when on.

A similar problem exists in the upconversion mixers, where it is desirable to maximize SNR in individual TX chains by maintaining strong TX signals. To further improve in-band swing in the upconversion mixer, the gates were DC coupled through a 2:1 resistive voltage divider to their respective baseband terminals, such that the gates partially track the baseband inputs, increasing signal handling by about 50% (Fig. 2c, [5]). Additionally, to minimize noise added by the PA pre-amp, an asymmetric, anti-phase pair of upconversion mixers were used to drive a push-pull PA driver (Fig. 2d).

B. Harmonic Predistortion

As shown in Fig. 2b, four resistive interpolation blocks were implemented in each TX upconversion chain. The first of these enables individual magnitude and phase control for each upconversion chain. The second is a similarly configured network that allows for injection of an additional baseband signal to perform in-band predistortion with a distinct distribution of amplitude and phase. The remaining two exploit harmonic conversion modes of the 8-phase upconversion mixer to inject second and third harmonic predistortion terms to cancel harmonics generated by the nonlinearity in the PA's.

Harmonic conversion can be achieved in 8-phase mixers by changing the effective phase of each baseband terminal depending on the harmonic to be upconverted. For the second harmonic, incrementing the baseband signals by 90° on each baseband port instead of the 45° used for the fundamental will result in operation identical to a 4-phase mixer with twice the LO frequency as shown in Fig. 2a. Since PA second harmonic terms will appear at $2F_{LO}+2F_{IF}$, second harmonic cancellation also requires a baseband input at $2F_{IF}$. Similarly, third harmonic can be generated with 135° phase increments and injecting at $3F_{IF}$ on each baseband port.

C. RX and TX Monitors

8-phase down-converting monitor circuits running on the TX LO are included at both ends of the distributed transmitter, providing direct access to the magnitude and phase of the TX signal at both ports, including 2nd and 3rd harmonics (Fig. 1). The ANT-end monitor has an attenuator to prevent saturation. On-chip monitors allow for quadrature, harmonic weight calculation from baseband signals without needing any external measurements or equipment.

D. Distributed Degeneration Network

While appropriate complex weighting of subtransmitters allows suppression of TX signals at the RX port, it does not provide rejection of noise and other perturbations in the individual transmit chains. In order to address this issue, [4] uses frequency-selective PA degeneration, which reduces PA noise in the RX band, but also greatly degrades output power when F_{TX} was placed too close to F_{RX}. Ideally sub-TX noise could be asymmetrically suppressed at the two ends of the transmission line similar to the TX signal. We achieve this by connecting the baseband terminals of the degeneration mixers to a shared bus. Complex weights are then applied to each degeneration mixer via a set of rotation multiplexers. Similar to

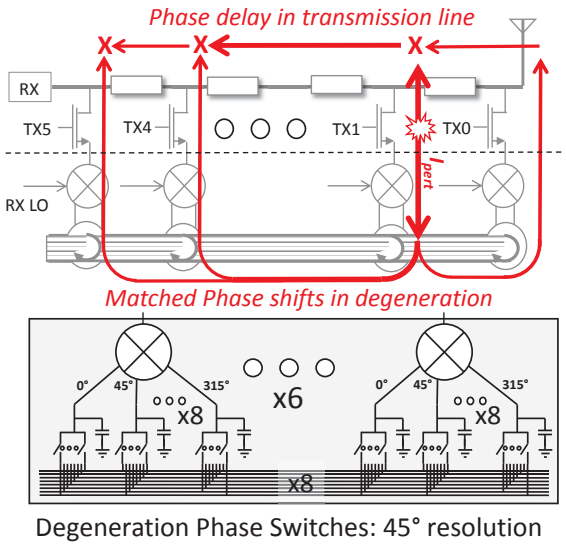

Fig. 3. Distributed degeneration. The tap weights can be chosen accordingly to suppress TX noise. Phase rotations in distributed degeneration match delay in transmission line.

suppression of the TX signal, appropriate selection of these complex weights suppresses noise at the receiver port without proportional TX gain suppression at the ANT port.

As shown in Fig. 3, complex weights were implemented by simple phase rotation. Switches steer the 8 baseband ports of each degeneration mixer to the shared bus in 45° steps. By steering the perturbations of any PA to the others with phase shifts that match those of the transmission line, the signal can be made to null at the receive port of the transmission line.

III. Measurement Results

A. Distributed Degeneration Measurements

To validate the proposed distributed degeneration approach, we compared different degeneration settings by looking at how signal injected from one PA travels differently to the antenna and receiver ports (Fig. 4). Compared to no degeneration, the individual degeneration technique from [4] recovers signal lost by the PA shunting and generates a notch at the RX frequency that reduces PA gain to both ports by >15dB compared to the out of band signal level.

Distributed degeneration has a similar impact on overall gain, and still produces a 12dB notch in PA gain to the RX port at the RX frequency, but now the PA gain to the antenna port actually slightly increases near the RX frequency.

B. Harmonic Predistortion Measurements

As shown in Fig. 5, for a fundamental output power of up to 18dBm, the second and third harmonic products can

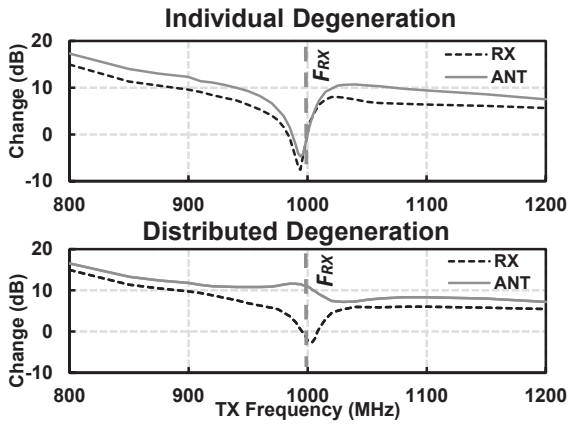

Fig. 4. Impact of different degeneration modes on single PA gain to RX and ANT ports. Y-Axis is change in amplitude relative to gain with no degeneration.

be suppressed to below -30dBm by predistortion, providing as much as 35dB improvement. Eventually the amount of baseband signal required to effectively null harmonics becomes greater than what the upconversion chain can supply, and so harmonic suppression degrades.

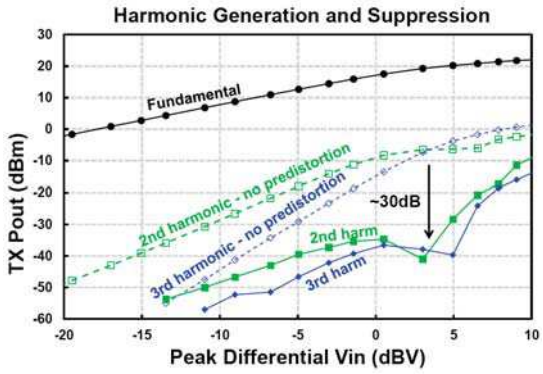

Fig. 5. Suppression of second and third harmonics.

C. Duplex Based Measurements

Fig. 6 shows the duplexing performance of this system for an RX frequency of 1GHz. In TDD mode, no PA degeneration is engaged, allowing for the maximum TX gain of greater than 16dB from 800MHz to 1.2GHz. Without degeneration, NF is degraded by over 15dB due to TX noise at the RX frequency. The baseline, TX-off RX noise figure is high due unexpected loss at the transmission line interface caused by mis-modeling of the transmission line itself. Engaging individual PA degeneration reduces TX gain, but improves RX NF degradation to only 5dB. For TX-RX spacing greater than 50MHz, TX gain stays

TABLE I
COMPARISON TO THE STATE OF THE ART

	[2]	[6]	[1]	[4]	**This Work**
Max TX Power	8dBm	10dBm	25dBm	19dBm	23dBm
Technology	65nm CMOS	65nm CMOS	40nm CMOS	65nm CMOS	28nm CMOS & 130nm SOI
Number of Antennas	1	2	1*	1	1
Operation Range	0.61-0.975GHz	0.15-3.5GHz	1.7-2.2GHz	0.3-1.6GHz	800-1.2GHz
TX/RX Isolation (Analog)	40dB	27dB	55dB	25dB	30-45dB
Area	0.94mm^2	2mm^2	3.5mm^2	12mm^2	23.1mm^2
*Requires connecting a circulator connecting TX-RX					

above 11dB under individual degeneration, but falls as low as 5dB for sub 50MHz spacing. TX gain at spacing under 50MHz can be partially recovered using distributed degeneration. In FD mode, TX gain improves to 9.5dB, while NF degradation is comparable to the individual degeneration case at less than 7dB. In all cases a TX-RX isolation of >30dB is preserved.

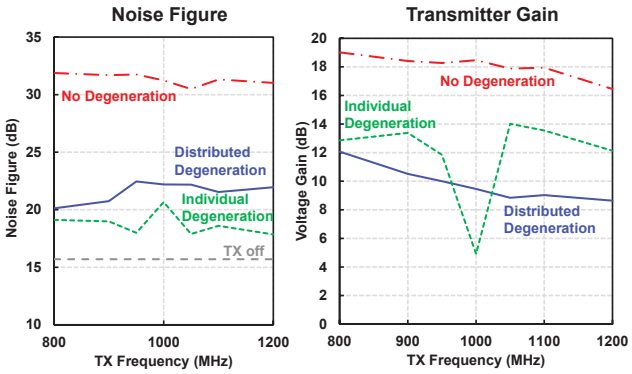

Fig. 6. Duplexing performance across different RX-TX spacing. In the individual degeneration case, R_{sw} of mixers degenerates the PA out of band, while in the no degeneration case we short out the mixer switches to present a low degeneration impedance.

IV. CONCLUSION

We demonstrated a dual-chip, integrated, and software-defined front end capable of supporting TDD, FDD, and FD modes (Fig. 7) where FD mode is enabled through a novel degeneration network. This technique improves upon transmit gain previously lost by frequency selective degeneration.

The effect of harmonic terms on the RX has not been previously addressed in similar duplexers. Here, we presented a predistortion scheme that can be used to mitigate TX nonlinearity, preventing RX saturation due to PA harmonics.

ACKNOWLEDGMENTS

This material is based in part upon work supported by the National Science Foundation under Grant No. 1641100. The authors would also like to thank Mark Rich, Michael Mack, MeeLan Lee, and Daniel Yetso from Google, Inc. for their support and insight. This paper is dedicated to the memory of Mark Rich, who was an early supporter of our ideas, and without whom this work may not have existed.

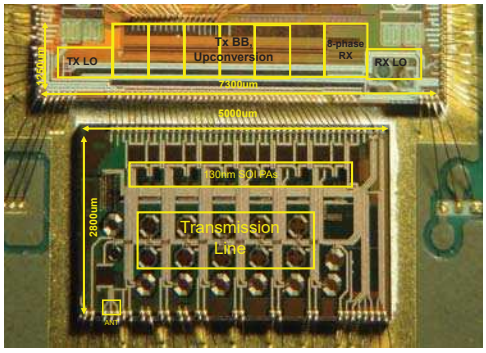

Fig. 7. Dual chip die photo. The bottom chip contains the PAs and the transmission line.

REFERENCES

[1] T. Zhang *et al.*, "A 1.7-to-2.2GHz full-duplex transceiver system with >50dB self-interference cancellation over 42MHz bandwidth," in *2017 IEEE ISSCC*, Feb. 2017, pp. 314–315.

[2] N. Reiskarimian *et al.*, "Highly-linear integrated magnetic-free circulator-receiver for full-duplex wireless," in *2017 IEEE ISSCC*, Feb. 2017, pp. 316–317.

[3] K. Fang and J. F. Buckwalter, "A tunable 5-7 GHz distributed active quasi-circulator with 18-dBm output power in CMOS SOI," *IEEE Microwave and Wireless Components Letters*, vol. 27, no. 11, pp. 998–1000, Nov. 2017.

[4] H. Yuksel *et al.*, "A wideband fully integrated software-defined transceiver for FDD and TDD operation," *IEEE JSSC*, vol. 52, no. 5, pp. 1274–1285, May 2017.

[5] D. J. van den Broek, E. A. M. Klumperink, and B. Nauta, "An in-band full-duplex radio receiver with a passive vector modulator downmixer for self-interference cancellation," *IEEE Journal of Solid-State Circuits*, vol. 50, no. 12, pp. 3003–3014, Dec 2015.

[6] D. J. van den Broek *et al.*, "A self-interference-cancelling receiver for in-band full-duplex wireless with low distortion under cancellation of strong TX leakage," in *2015 IEEE ISSCC*, Feb. 2015, pp. 1–3.